Crystallization of pyroxenes in an iron-rich diabase from Minnesota.

By I. D. MUIR, B.A., Ph.D., F.G.S.

Department of Mineralogy and Petrology, University of Cambridge.

[Read November 5, 1953.]

THE Beaver Bay diabase forms an irregular sill-like intrusion about 3000 feet in thickness exposed over a distance of approximately six miles from Split Rock to Beaver Bay on the north shore of Lake Superior, Minnesota. It is intrusive into the Keeweenaw volcanic series above the Duluth gabbro to which it is almost certainly related. It is the largest of many such sills in this region and includes several petrographic facies grading from troctolite, through olivine-gabbro, normal gabbro, and ferrogabbro to red granite.

Analyses of several types of diabase from the Minnesota coast near Beaver Bay are given by Grout and Schwartz (1939) and include one of the iron-rich facies (table I, anal. 3) collected from Highway 61 about $1\frac{1}{4}$ miles SW. of the Beaver Bay settlement. A similar rock (table I, anal. 2) collected from the roadside about $\frac{5}{8}$ mile nearer Beaver Bay settlement and kindly supplied by Dr. F. Grout, exhibits several petrographic features worthy of comment. Tilley (1950) has drawn attention to the similarity between the fractionation in this diabase and that of the Skaergaard intrusion (Wager and Deer, 1939). For comparison a new analysis is given (table I, no. 1) of a Skaergaard ferrohortonolite-ferrogabbro showing similar iron enrichment to the Beaver Bay rock.

The analysed specimen of the Beaver Bay rock (table I, anal. 2) is a mesotype, rather coarse-grained diabase composed chiefly of clear subhedral plagioclase, rounded grains of fayalitic olivine, and three pyroxenes occurring either as stout subhedral grains up to one millimetre in length (ferroaugite) or as clusters of smaller anhedral grains composed of all three pyroxenes associated with olivine and iron-ores. Apatite, sometimes pigmented, is a prominent accessory, magnetite and ilmenite are the principal ores, and pyrrhotine is sometimes present as lamellae intergrown with the magnetite. Interstitially a little quartz is found in micrographic intergrowth with oligoclase and potash-felspar.

The plagioclase (An_{44}) occurs as subhedral grains up to two millimetres in length which are practically unzoned, and twinned chiefly after the albite, Carlsbad, albite-Carlsbad, and pericline laws. Strong marginal zoning to oligoclase (An_{20}) is exhibited by crystals adjoining the quartzo-felspathic mesostasis.

TABLE I. Rock analyses.

	1.	2.	3.	4.
SiO_2 ...	43·05	45·87	45·84	52·41
Al_2O_3 ...	10·58	10·66	11·19	12·23
Fe_2O_3 ...	4·49	4·11	4·02	3·53
FeO ...	18·23	15·59	16·30	12·86
MgO ...	3·92	3·50	3·66	2·62
CaO ...	10·37	8·28	8·39	8·48
Na_2O ...	3·20	2·84	2·68	2·01
K_2O ...	0·60	0·96	0·83	0·85
H_2O+ ...	0·11	1·42	0·87	0·92
H_2O- ...	0·16	0·47	0·45	0·14
TiO_2 ...	2·54	4·65	3·44	3·14
P_2O_5 ...	2·95	1·70	1·74	0·23
MnO ...	0·22	0·29	0·27	0·26
S ...	—	—	0·04	—
CO_2 ...	—	—	—	0·12
	100·42	100·34	99·72	99·80

Norms.

		1.	2.	3.	4.
	Q	—	2·58	1·74	12·82
	Or	3·34	6·12	5·00	5·28
	Ab	27·25	24·10	23·06	16·87
	An	12·79	13·34	15·85	21·85
Di	Wo	8·12	6·96	6·15	7·71
	En	4·00	8·70	9·20	6·55
	Fs	10·69	18·08	20·86	15·91
Ol	Fo	4·06	—	—	—
	Fa	11·42	—	—	—
	Il	4·86	8·82	6·54	5·99
	Mt	6·50	6·03	5·80	5·17
	Ap	7·06	4·03	4·03	0·37

Normative pyroxene.

	1.	2.	3.	4.
Wo ...	35·6	20·7	17·1	25·6
En ...	17·5	25·8	25·4	21·4
Fs ...	46·9	53·5	57·5	53·0

$$\frac{FeO+Fe_2O_3\times 100}{MgO+FeO+Fe_2O_3}$$

	1.	2.	3.	4.
Ferroaugite	72	69	—	—
Rock ...	86	89	86	82

1. Ferrohortonolite-ferrogabbro EG 4272. Skaergaard intrusion, east Greenland. Analyst, I. D. Muir.
2. Iron-rich diabase M3174 Highway 61. Five-eighths mile S.W. of settlement Beaver Bay, Minnesota. Analyst, J. H. Scoon.
3. Iron-rich diabase Highway 61 (Grout and Schwartz, 1939, table II, anal. 2). Analyst, R. B. Ellestad.
4. Iron-rich dolerite EH52 of New Amalfi intrusive sheet, South Africa. (Poldervaart, 1944, table VI.) Analyst, W. H. Herdsman.

Olivine (Fa_{80}), occurring as small rounded and partly resorbed grains (table II, anal. 2), has an unusual habit for such an iron-rich member of the series. It has ceased crystallizing at a relatively early stage and is invariably surrounded either by a reddish-brown highly-birefringent alteration product which is mostly bowlingite, or, more rarely, by deep-green isotropic chlorophaeite. Sometimes the olivine is enclosed by a pyroxene or stout grains of magnetite, but the thin mantle of bowlingite always intervenes.

Three distinct pyroxenes occur, ferroaugite, pigeonite, and hypersthene. Ferroaugite, which is the most abundant, is practically unzoned, and is sometimes mantled abruptly by pigeonite or hypersthene, but the reverse is also found. It is pinkish in colour, subophitic in habit, and exhibits two sets of very fine exsolution lamellae. The lamellae parallel to (100) are probably of hypersthene (Poldervaart and Hess, 1951); and the second set, extremely fine lamellae parallel to (001), have the same optical orientation as any mantling pigeonite. The ferroaugite sometimes mantles the olivine, but there is no suggestion of a reaction relationship.

TABLE II. Mineral analyses.

	Mineral analyses.				Atoms on basis of 6 oxygens.		Atoms on basis of 4 oxygens.
	A.	1.	2.		A.	1.	2.
SiO_2	47·70	48·86	30·42	Si	1·886	1·906	0·968
Al_2O_3	1·55	1·51	0·50	Al	0·074	0·071	0·019
TiO_2	1·24	0·93	1·20	Ti	0·037	0·023	—
Fe_2O_3	1·82	2·26	nil	Al	—	—	—
FeO	20·32	18·71	57·62	Ti	—	0·005	0·038
MnO	0·38	0·38	n. d.	Fe'''	0·049	0·066	—
MgO	8·73	9·48	8·17	Fe''	0·672	0·608	1·526
CaO	17·32	17·58	1·32	Mn	0·012	0·014	—
Na_2O	0·65	0·24	n. d.	Mg	0·520	0·550	0·389
K_2O	0·13	nil	n. d.	Ca	0·736	0·735	0·044
H_2O+	0·21	0·25	0·18	Na	0·050	0·019	—
H_2O-	0·11	0·06	0·21	K	0·007	—	—
	100·16	100·26	99·62	z	2·00	2·00	0·99
				$X+Y$	2·05	2·00	2·00

A. Ferroaugite from ferrohortonolite-ferrogabbro EG 4272. Skaergaard intrusion. (Muir, 1951, table II, no. 14.)

1. Ferroaugite from iron-rich diabase (M3174), Beaver Bay. Analyst, I. D. Muir.
2. Olivine from same. Analyst, I. D. Muir.

Unlike the ferroaugite, the pigeonite occurs rarely as discrete crystals, but is found mostly as mantles to the lime-rich clinopyroxene or as a constituent of the clusters of ferromagnesian minerals, where it is frequently associated with the inverted orthopyroxene; both minerals may enclose olivine. It varies little in refractive index but the optic axial angle ranges 0–10° in different grains with the optic axial plane parallel to (010). Conspicuous exsolution lamellae of augite developed parallel to (001) are much coarser than the corresponding pigeonite lamellae found in the accompanying ferroaugite—an unusual feature.

Hypersthene (orthoferrosilite, Of_{74}), with sheets of ferroaugite inclusions parallel to (001) of the original clinopyroxene, is more abundant than pigeonite. It tends to occur mostly in the clusters of ferromagnesian crystals, but is sometimes found as large crystals mantling the ferroaugite. Where such hypersthene adjoins the late mesostasis it is frequently mantled by a primary orthopyroxene (Of_{75}) with very fine exsolution lamellae of augite developed parallel to (100). In such circumstances the orthopyroxene is not infrequently associated with a brown hornblende or intergrown with skeletal ilmenite.

Some composite pyroxene grains display relics of pigeonite enclosed in a single crystal of inverted hypersthene (fig. 1A). The parallelism of the crystals, the similarity of textures, and the identity of the bulk composition of the hypersthene (from a partial analysis) with that deduced optically for the pigeonite, indicates that most of the original pigeonite of the rock has inverted to hypersthene and that in this process coarse lamellae of ferroaugite were exsolved. These are continuous with the finer lamellae in the residual pigeonite. As most of the remaining pigeonite occurs either as small crystals intergrown with ferroaugite or as narrow mantles thereto, it would appear that the stable augite framework has tended to preserve the pigeonite, because of the parallelism and similarity of the two structures. Hess and Henderson (1949) have described a somewhat similar case where a small proportion of the pigeonite of a meteorite has inverted to orthopyroxene and the remainder exhibits very broad exsolution lamellae of augite.

From the very fine nature of the exsolution lamellae in the ferroaugite of this rock and the inversion of part only of the pigeonite, it can be inferred that cooling in the Beaver Bay sill was more rapid than that of comparable rocks of the Skaergaard intrusion where exsolution lamellae of pigeonite in the ferroaugite are much coarser. Hypersthene lamellae parallel to (100) are seen only in the early magnesian clinopyroxenes from the Skaergaard hypersthene-olivine-gabbros. In the Skaergaard clinopyroxenes of the middle and ferrogabbros, exsolution took place while the temperature was still above the pigeonite–orthopyroxene inversion, but in the Beaver Bay rocks with more rapid cooling only a little pigeonite was able to exsolve above the inversion temperature and the remaining excess of the lime-poor phase has separated as hypersthene lamellae parallel to (100). Optical data for these minerals are listed in table III.

The closest chemical comparison with the two analyses of iron-rich Beaver Bay diabases is a ferrohortonolite-ferrogabbro (table I, anal. 1)

FIG. 1. Iron-rich diabase of Beaver Bay, Minnesota.

A. Composite grain in centre of field shows a resorbed crystal of fayalitic olivine altered marginally to bowlingite, enclosed in a large crystal of inverted orthopyroxene with some of the original pigeonite remaining. On the left side of the field a little ferroaugite mantles the olivine. Iron-ore and pigmented apatite are prominent accessories.

B. i. (upper left).—Resorbed olivine with bowlingite mantle enclosed by pigeonite intergrown with ilmenite. The pigeonite in turn is enclosed by ferroaugite. ii. (upper right).—Ferroaugite with feeble exsolution lamellae parallel to (001) is margined by a narrow rim of pigeonite showing conspicuous exsolution lamellae. Olivine on extreme right has a broad mantle of inverted orthopyroxene enclosing relics of pigeonite. Inverted hypersthene in the upper part of the field has a clear margin of primary hypersthene adjacent to the quartzo-felspathic mesostasis. Much of the late plagioclase is antiperthitic. iii. (lower portion).—Large crystal of ferroaugite and a smaller grain of pigeonite, part of which has inverted to hypersthene with sheets of clinopyroxene inclusions. The pyroxenes are set in a base of bowlingite derived from the olivine.

of the Skaergaard intrusion. As the Beaver Bay rocks are considerably poorer in lime than the Skaergaard ferrogabbros and carry a more basic plagioclase, their normative pyroxenes are much poorer in lime and pigeonites are present in the iron-rich facies, whereas in the Skaergaard intrusion, lime-poor pyroxenes have ceased to form much above the base of the ferrogabbros. Like the analysed Skaergaard rock, the iron-rich Beaver Bay diabases are very high in phosphorus. Analyses of more magnesian types from the intrusion are very low in this constituent

TABLE III. Optical properties and compositions of pyroxenes and associated olivines.

	1.	2.	3.	4.	5.	6.	7.	8.	9.
α	1·718	—	1·704	1·729	1·741	1·787	1·711	—	—
β	1·725	1·818	1·711	1·730	1·750	1·821	1·716	—	—
γ	1·741	—	1·733	1·757	1·757	1·838	1·738	—	—
2V	52°	58°	50°	0–10°	65°	58–56°	46–56° av. 49°	64–67° av. 66·5°	54·5°
γ:c	43°	—	39°	40°	—	—	43°	—	—
Colour ...	brownish	pale yellow	brownish	pale yellow-green	pale green	pale yellow	brownish	pale green	pale yellow
Pleochroism	feeble	none	feeble	feeble	feeble	none	feeble	feeble	none
Composition atomic % Ca	37	—	38	9	—	2	37	—	—
Mg	26	22	28	27	25	20	27	27	15
Fe	37	78	34	64	75	78	36	73	85

Values of all refractive indices ±0·002. 2V and extinction angles γ:c ±2°.

1. Ferroaugite from ferrohortonolite-ferrogabbro EG 4272. (Table I, anal. 1.) Skaergaard intrusion.
2. Olivine from same.
3. Ferroaugite from iron-rich diabase M3174 Beaver Bay. (Table I, anal. 2.)
4. Pigeonite from same.
5. Hypersthene from same.
6. Olivine from same.
7. Ferroaugite from iron-rich dolerite EH52. (Table I, anal. 4.) New Amalfi intrusive sheet, South Africa.
8. Hypersthene from same.
9. Olivine from same.

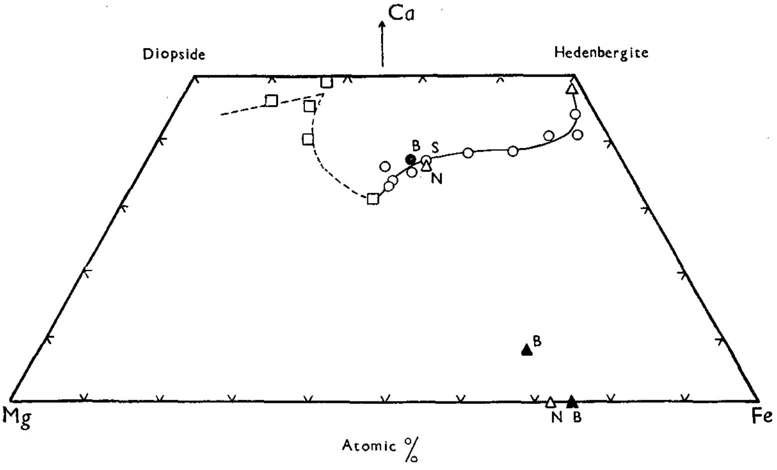

FIG. 2. Pyroxenes from the Beaver Bay diabase.

Comparison is made with the Skaergaard normal clinopyroxene trend (Muir, 1951) and with the pyroxenes in an iron-rich dolerite from New Amalfi, South Africa.

○ ● Analysed pyroxenes. □ Clinopyroxene composition recalculated from analysis of bulk pyroxene of the rock. ▲ △ Composition estimated from optical properties. B = Beaver Bay pyroxenes. N = New Amalfi pyroxenes. S = Skaergaard ferroaugite (table II, anal. 1).

and it would appear that here as with the Skaergaard example the phosphorus content of the magma increased until it was saturated and then apatite appeared suddenly as a major constituent.

The compositions of the ferromagnesian silicate minerals of the Beaver Bay and Skaergaard rocks are plotted in fig. 2 along with those from a comparable iron-rich dolerite of the New Amalfi intrusive sheet, South Africa (Poldervaart, 1944). From this, and the data of table IV, it can be seen that the distribution of iron and magnesium between the different associated minerals follows a generally similar pattern although the olivine of the Beaver Bay diabase is of early formation, whereas in the other cases it formed after the ferroaugite. It is also of interest to note that both the Beaver Bay and New Amalfi ferroaugites lie on the Skaergaard trend (Muir, 1951).

TABLE IV. Iron enrichment in associated ferromagnesian minerals.

	$\frac{\text{Fe}}{\text{Fe+Mg}}$ atomic %.		
	1.	2.	3.
Augite	59	55	57
Pigeonite	—	71	—
Hypersthene	—	75	73
Olivine	78	79·5	85

1. Skaergaard ferrogabbro (table I, anal. 1).
2. Beaver Bay diabase (table I, anal. 2).
3. New Amalfi iron-rich dolerite (table I, anal. 4).

The compositions of associated orthopyroxenes, pigeonites, and augites taken mostly from Kuno's work are plotted in fig. 3. From this it can be seen that the usual relationship is for the pigeonite to be slightly more iron-rich than its associated orthopyroxene. Using the data for the analysed pyroxene pair H_2–H_3 in the diagram, Kuno and Nagashima (1952) have been able to deduce the magnitude of the pigeonite–orthopyroxene inversion interval at one point. The reversal of the usual relationship in the case of the Beaver Bay rock supports the textural evidence that this primary hypersthene formed later and at a lower temperature than the pigeonite.

It is also of interest to compare the relative iron-enrichment of the associated orthopyroxenes and olivines. The data of table IV agree with the work of Bowen and Schairer (1935) who found that in synthetic pairs the olivine was always the more iron-rich, a relationship which was the reverse of what commonly obtains in igneous rocks. They attributed the difference to the order of crystallization of the different minerals in basic igneous rocks, where a magnesian olivine when present is usually the earliest mineral to separate.

Ramberg and De Vore (1951) have collected data on natural olivine-orthopyroxene pairs and shown that the iron-rich minerals conform to the synthetic pattern, but that for their Wyoming syenites the difference in iron-enrichment is greater on the average than for synthetic pairs. Within the magnesian range, however, they confirmed Bowen and Schairer's observations. Later, Ramberg (1952) discussed on theoretical grounds the distribution of iron and magnesium in coexisting olivines and orthopyroxenes and considered that the relative enrichment in iron shown by the olivines could be attributed to the lower average electronegativity of the oxygen forming the metal-oxygen bonds in the orthosilicate. The presence of more tetrahedrally co-ordinated aluminium in an augite would on this theory make it more receptive to

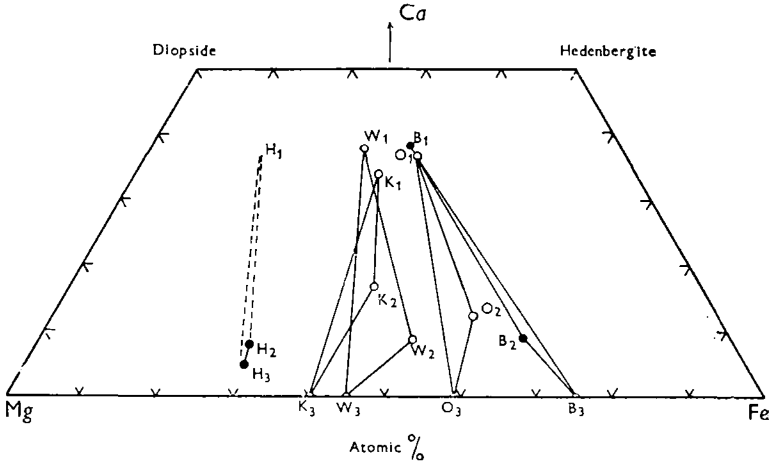

FIG. 3. Associated pyroxenes from 3-pyroxene rocks.

B. Beaver Bay diabase: B_1 ferroaugite (anal.), B_2 pigeonite, B_3 primary orthopyroxene.

H. Hakone andesite (Kuno and Nagashima, 1952): H_2 pigeonite (anal.), H_3 orthopyroxene (anal.), H_1 inferred composition of associated augite.

K. Hakone andesite (Kuno, 1936. Jap. Journ. Geol. Geogr., vol. 13, p. 125): K_1 augite, K_2 pigeonite, K_3 orthopyroxene.

O. Okuba Yama andesite (Kuno and Inoue, 1949. Proc. Jap. Acad., vol. 25, no. 4, pp. 128–132): O_1 ferroaugite, O_2 pigeonite, O_3 orthopyroxene.

W. Weiselbergite (Kuno, 1947. Proc. Jap. Acad., vol. 23, no. 9, p. 111): W_1 augite, W_2 pigeonite, W_3 orthopyroxene.

iron-enrichment than an associated orthopyroxene, but the reverse is always the case.

The two-pyroxene boundary.

All three rocks whose pyroxenes are plotted in fig. 2 appear to have formed from liquids lying close to the two-pyroxene boundary. In the case of the Skaergaard rocks, lime-poor pyroxene ceased to form only slightly later than the reappearance of olivine, and there is no evidence of a reaction relation with ferriferous olivine being responsible for the final disappearance of this pyroxene (Muir, 1951). In the Beaver Bay rocks, olivine of early formation is mantled frequently by pigeonite or its inverted equivalent. In the New Amalfi rock both the olivine and orthopyroxene have formed about the same time at a very late stage and there is no evidence of a reaction relation between them. It would appear, therefore, that the disappearance of the lime-poor pyroxene in iron-rich tholeiitic rocks could not be due to a reaction relation with fayaltic olivine.

Another suggestion which has been advanced to account for the presence of only one pyroxene (ferroaugite) in the later stages, in place of the two which are found in the earlier rocks of some intrusions, is that when the two-pyroxene boundary is approached, the binary cotectic relationship of limited solid solution between augite and pigeonite develops into a solid-solution series with a minimum and the augite and pigeonite compositions converge, one becoming more lime-poor and the other richer in lime. However, the ferroaugites associated with pigeonite are now known to become progressively more lime-rich, and this does not conform well to a change over to a complete solid-solution relationship with a minimum.

If neither of these hypotheses are accepted it must follow that minerals of the pigeonite series should continue to form as long as the composition of the magma permitted and that any disappearance of the lime-poor pyroxene phase would be due to some change in the composition of the magma towards the lime-rich side of the pyroxene field.

A new hypothesis advanced here to explain the rather complex pyroxene relations near the two-pyroxene boundary can best be illustrated by a series of hypothetical phase diagrams (fig. 4) at different stages of iron-enrichment across the pyroxene field. For this purpose the simple binary diagram alone is rather misleading because the liquidus will always be enriched in iron with respect to the solidus and

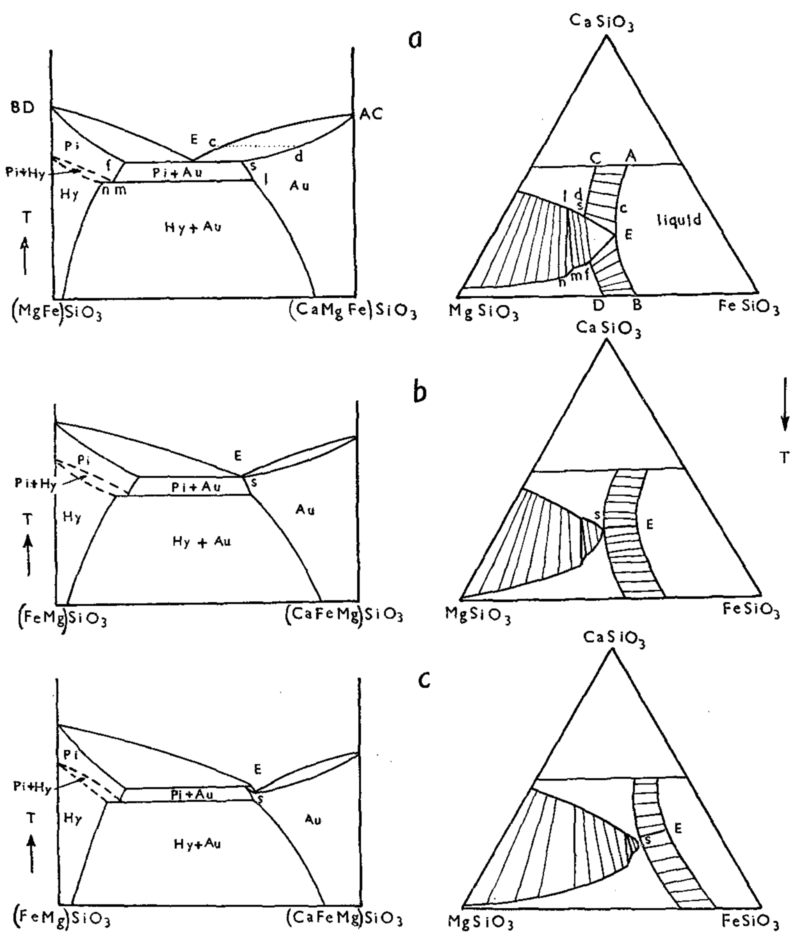

FIG. 4. Hypothetical equilibrium diagrams for pyroxenes.

The diagrams on the left represent the phase relations in a simplified manner as a pseudo-binary system. Diagrams on the right show hypothetical phase equilibria for a series of isothermal planes at successively lower temperatures and at different stages of iron-enrichment.

(*a*) Two-pyroxene field. The diagram on the right represents an isothermal plane at the temperature of the line *fEs* of the left-hand diagram. From a liquid of composition *c*, augite *d* would crystallize. If the liquid has a composition *E* on the pyroxene cotectic curve, two pyroxenes *f* (pigeonite) and *s* (augite) should separate. On the right-hand diagram the triangle *lmn* represents the pigeonite–hypersthene inversion-interval. Comparable points in the two diagrams are designated by the same letter.

(*b*) Limit of two-pyroxene field. The cotectic curve at *E* has migrated to the lime-rich side of the intersection with the solvus. From liquid *E*, a single pyroxene *s* of similar lime-content will separate. Right-hand diagram represents the isothermal plane of temperature *Es* on left-hand diagram.

(*c*) One-pyroxene field. The cotectic curve at *E* has become detached from the solvus, and ferroaugite *s* alone should separate from the liquid. Right-hand diagram represents the isothermal plane of temperature *Es* on left-hand diagram.

the two coexisting pyroxene phases will have different iron-magnesium ratios. The diagrams used to illustrate pyroxene relations in the central part of the system include a set showing relations for a series of isothermal planes with falling temperature.

The subsolidus relations for the system $Mg_2Si_2O_6$–$CaMgSi_2O_6$ have been determined by Atlas (1952) who has found that the maximum on the solvus appears to lie only very slightly below the solidus located by Bowen (1914). Thus, in the synthetic dry system, there is a simple solid-solution series with a minimum, but any addition of a little water or other constituents to the liquid would almost certainly lower the minimum, enabling the solvus to cut the solidus and produce two immiscible series of pyroxenes. With iron entering the system the maximum of the solvus should not fall as rapidly as the liquidus, and two pyroxenes would continue to separate (fig. 4*a*).

As the limit of the two-pyroxene field is approached it seems probable that the minimum of the liquidus would migrate towards the lime-rich side of its intersection with the solvus (fig. 4*b*). This should cause the proportion of lime-poor pyroxene to diminish very gradually as seems to be the case in the latest two-pyroxene rocks of the Skaergaard intrusion. When the minimum passes beyond the limit of the intersection with the solvus (fig. 4*c*) the lime-poor pyroxene should cease to separate as a separate phase, although it could still appear as exsolution lamellae in the ferroaugite on slow cooling. In different magmas the position and temperature of the minimum would vary somewhat according to the amounts of other constituents in the magma, and hence the limit of the two-pyroxene field in different magmas could occur at slightly differing iron-magnesium ratios.

Such a hypothesis could account for the disappearance of pigeonite in iron-rich tholeiitic rocks, but in some of these a primary hypersthene is present in the late crystallizing material along with augite and iron-ore. From the presence of exsolved hypersthene in the ferroaugite of the Beaver Bay diabase and of a primary hypersthene in the late crystallizing material it may be inferred that the bulk of the rock formed at a temperature not greatly in excess of the hypersthene–pigeonite inversion. An increased content of volatiles in the iron-enriched interstitial liquid could lower the crystallization temperature of the minimum below that of the hypersthene–pigeonite inversion. For rocks which have formed from liquids just beyond the limit of the two-pyroxene field (fig. 4*c*) the minimum could now once again intersect the solvus, and result in two pyroxenes (ferroaugite and hypersthene) appearing again in the residuum. This seems to be the explanation of the hypersthene in the New Amalfi rock.

Strong zoning of moderately iron-rich augites towards subcalcic augite and lime-rich pigeonite [optic axial plane (010)] has been reported from some of the Karroo dolerites (Walker and Poldervaart, 1949), Central Australian dolerites (Wilson, 1948), NE. Otago tholeiites (Benson, 1944), and Japanese andesites (Kuno, 1936). This type of zoning is relatively uncommon and in this case it would appear that the pyroxene cotectic curve has migrated towards the lime-poor side of its intersection with the solvus and that crystallization must have been effected at rather elevated temperatures. Here then, at a medium stage of iron-enrichment, it seems that alternative trend lines are possible for tholeiitic pyroxenes, one type leading towards the relatively lime-rich ferroaugites and the other to pigeonitic types. For more extremely iron-enriched liquids the pyroxene relations may be complicated by the formation initially of iron-wollastonites such as were recognized in the Skaergaard intrusion by Wager and Deer (1939), and which, perhaps also, may have formed in the most iron-rich rocks of the New Amalfi intrusive sheet.

The author wishes to express his gratitude to Professor C. E. Tilley for drawing his attention to the problems presented by the Beaver Bay pyroxenes, and for advice and criticism of this paper. To Professor J. B. Thomson also thanks are due for helpful discussions on pyroxene problems. Professors F. Walker and A. Poldervaart very kindly supplied specimens of the New Amalfi rocks, and Mr. J. H. Scoon carried out an analysis of the diabase specimen from Beaver Bay which is published here by courtesy of Professor Tilley.

References.

Atlas (L.), 1952. The polymorphism of $MgSiO_3$ and solid-state equilibria in the system $MgSiO_3$–$CaMgSi_2O_6$. Journ. Geol., vol. 60, pp. 125–147. [M.A. **12**–80.]

Benson (W. N.), 1944. The basic igneous rocks of eastern Otago and their tectonic environment. Part IVb. Trans. Roy. Soc. New Zealand, vol. 74, pp. 71–123. [M.A. **9**–151.]

Bowen (N. L.), 1914. The ternary system: diopside–forsterite–silica. Amer. Journ. Sci., ser. 4, vol. 38, pp. 207–264.

—— and Schairer (J. F.), 1935. The system MgO–FeO–SiO_2. Amer. Journ. Sci., ser. 5, vol. 29, pp. 151–217. [M.A. **6**–352.]

Grout (F. F.) and Schwartz (G. M.), 1939. The geology of the anorthosites of the Minnesota coast of Lake Superior. Bull. Minnesota Geol. Surv., no. 28. [M.A. **8**–242.]

Hess (H. H.) and Henderson (E. P.), 1949. The Moore County meteorite: a further study with comment on its primordial environment. Amer. Min., vol. 34, pp. 494–507.

Kuno (H.), 1936. On the crystallization of pyroxenes from rock-magmas, with special reference to the formation of pigeonite. Japanese Journ. Geol. Geogr., vol. 13, pp. 141–150. [M.A. **6**–295.]

—— and Nagashima (K.), 1952. Chemical compositions of hypersthene and pigeonite in equilibrium in magma. Amer. Min., vol. 37, pp. 1000–1006. [M.A. **12**–138.]

Muir (I. D.), 1951. The clinopyroxenes of the Skaergaard intrusion, eastern Greenland. Min. Mag., vol. 29, pp. 690–714.

Poldervaart (A.), 1944. The petrology of the Elephant's Head dike and the New Amalfi sheet (Matatiele). Trans. Roy. Soc. South Africa, vol. 30, pp. 85–119.

—— and Hess (H. H.), 1951. Pyroxenes in the crystallization of basaltic magma. Journ. Geol., vol. 59, pp. 472–489. [M.A. **11**–490.]

Ramberg (H.), 1952. Chemical bonds and distribution of cations in silicates. Journ. Geol., vol. 60, pp. 331–355. [M.A. **12**–27.]

—— and DeVore (G.), 1951. The distribution of Fe^{++} and Mg^{++} in coexisting olivines and pyroxenes. Journ. Geol., vol. 59, 193–210. [M.A. **11**–390.]

Tilley (C. E.), 1950. Some aspects of magmatic evolution. Quart. Journ. Geol. Soc., vol. 106, pp. 37–61. [M.A. **11**–394.]

Wager (L. R.) and Deer (W. A.), 1939. Geological investigations in east Greenland. Part III. The petrology of the Skaergaard intrusion, Kangerdlugssuaq, east Greenland. Meddel. om Grønland, vol. 106, no. 4, pp. 1–352. [M.A. **8**–27.]

Walker (F.) and Poldervaart (A.), 1949. Karroo dolerites of the Union of South Africa. Bull. Geol. Soc. Amer., vol. 60, pp. 591–705. [M.A. **11**–32.]

Wilson (A. F.), 1948. The charnockitic and associated rocks of north-western South Australia. Part II. Trans. Roy. Soc. South Australia, vol. 72, pp. 178–200. [M.A. **11**–151.]